·Article·
Advances in Polar Science
doi: 10.13679/j.advps.2018.2.00108
June 2018 Vol. 29 No. 2: 108-117

U-Th-Pb monazite and Sm-Nd dating of high-grade rocks from the Grove Mountains, East Antarctica: further evidence for a Pan-African-aged monometamorphic terrane

LIU Xiaochun[1*], LING Xiaoxiao[2] & JAHN Bor-ming[3]

[1] Institute of Geomechanics, Chinese Academy of Geological Sciences, Beijing 100081, China;
[2] Institute of Geology and Geophysics, Chinese Academy of Sciences, Beijing 100029, China;
[3] Department of Geological Sciences, National Taiwan University, Taipei 10699, China

Received 4 April 2018; accepted 14 June 2018

Abstract The Grove Mountains, 400 km south of the Chinese Antarctic Zhongshan Station, are an inland continuation of the Pan-African-aged (i.e., Late Neoproterozoic/Cambrian) Prydz Belt, East Antarctica. In this paper we carried out a combined U-Th-Pb monazite and Sm-Nd mineral-whole-rock dating on para- and orthogneisses from bedrock in the Grove Mountains. U-Th-Pb monazite dating of a cordierite-bearing pelitic paragneiss yields ages of 523 ± 4 Ma for the cores and 508 ± 6 Ma for the rims. Sm-Nd mineral-whole-rock isotopic analyses yield isochron ages of 536 ± 3 Ma for a coarse-grained felsic orthogneiss and 507 ± 30 Ma for a fine-grained quartzofeldspathic paragneiss. Combined with previously published age data in the Grove Mountains and adjacent areas, the older age of ~530 Ma is interpreted as the time of regional medium- to low-pressure granulite-facies metamorphism, and the younger age of ~510 Ma as the cooling age of the granulite terrane. The absence of evidence for a Grenville-aged (i.e., Late Mesoproterozoic/Early Neoproterozoic) metamorphic event indicates that the Grove Mountains have experienced only a single metamorphic cycle, i.e., Pan-African-aged, which distinguishes them from other polymetamorphic terranes in the Prydz Belt. This will provide important constraints on the controversial nature of the Prydz Belt.

Keywords **U-Th-Pb monazite dating, Sm-Nd mineral-whole-rock dating, Pan-African-aged, Grove Mountains, East Antarctica**

Citation: Liu X C, Ling X X, Jahn B-M. U-Th-Pb monazite and Sm-Nd dating of high-grade rocks from the Grove Mountains, East Antarctica: further evidence for a Pan-African-aged monometamorphic terrane. Adv Polar Sci, 2018, 29 (2): 108-117, doi:10.13679/j.advps.2018.2.00108

1 Introduction

Discovery of the Pan-African-aged (i.e., Late Neoproterozoic/Cambrian, ~550–500 Ma) high-grade tectonothermal event in Prydz Bay, East Antarctica (Fitzsimons et al., 1997; Carson et al., 1996; Hensen and Zhou, 1995; Zhao et al., 1995, 1992) constituted one of the most important steps in understanding Antarctic geology and led to recognizing a new orogen, termed the Prydz Belt (Zhao et al., 2003; Fitzsimons, 2000) or Kuunga Orogen (Boger, 2011), in the interior of what had been considered a single continent, East Gondwana. However, since the Pan-African-aged event in the Prydz Belt overprinted not only the Grenville-aged (i.e., Late Mesoproterozoic/Early Neoproterozoic, ~1000–900 Ma) Rayner Complex, but also Archean-Paleoproterozoic cratonic blocks, there has been an extended debate on the

* Corresponding author, E-mail: liuxchqw@cags.ac.cn

extent, process and role of both Grenville-aged and Pan-African-aged tectonothermal events, which has resulted in several models for reassembling Rodinia and Gondwana (Fitzsimons, 2003; Harley, 2003; Yoshida et al., 2003; Zhao et al., 2003).

The Grove Mountains, situated about 400 km south of Prydz Bay (Figure 1a), are considered as an inland continuation of the Prydz Belt (Liu et al., 2003a, 2002; Zhao et al., 2003, 2000; Mikhalsky et al., 2001b). U-Pb zircon analyses for bedrock from the Grove Mountains revealed an Early Neoproterozoic mafic and felsic igneous intrusion and a Pan-African-aged granulite-facies metamorphism and widespread charnockitic and granitic magmatism (Liu et al., 2007a, 2006; Zhao et al., 2003). Zircons from glacial moraines collected from the Grove Mountains also only record a Pan-African-aged metamorphic event (Hu et al., 2016; Wang et al., 2016a, 2016b; Liu et al., 2009a). In order to further examine the question on whether the Grove Mountains have experienced only a single Pan-African-aged metamorphic cycle, or represent a polymetamorphic terrane as other parts of the Prydz Belt, we carried out a combined U-Th-Pb monazite and Sm-Nd mineral-whole-rock dating on para- and orthogneisses from bedrock. The results support the suggestion that the Grove Mountains are a Pan-African-aged monometamorphic terrane in the Prydz Belt (Liu et al., 2013).

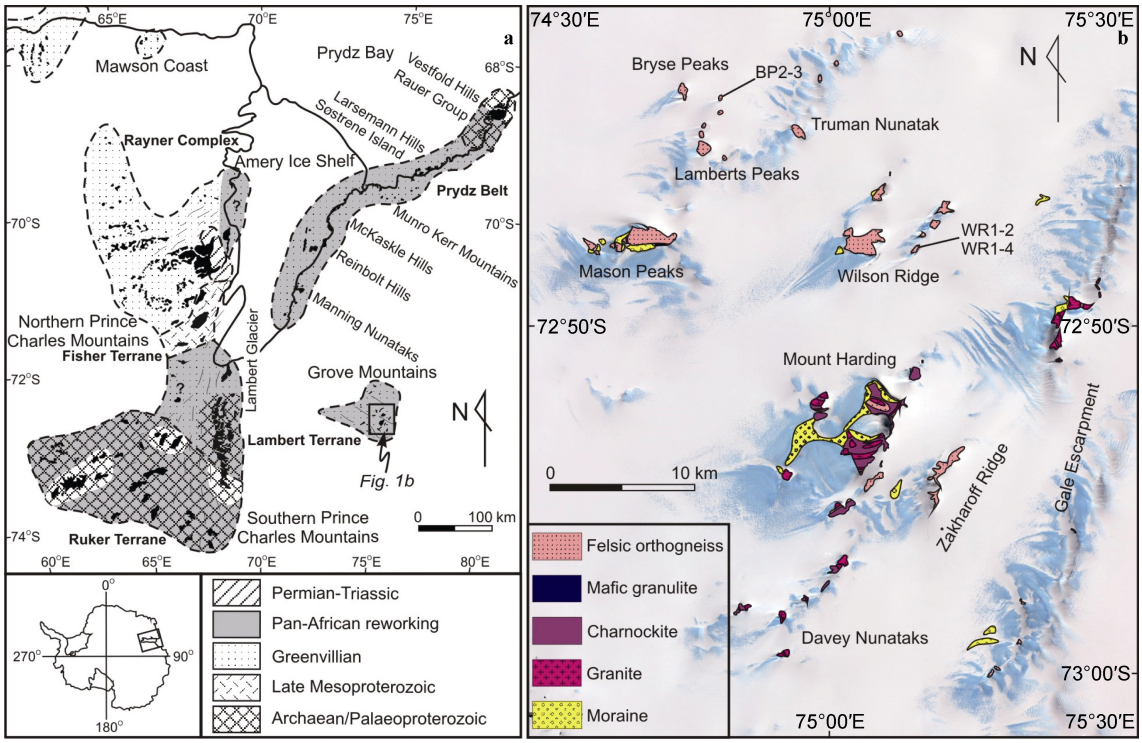

Figure 1 **a**, Geological sketch map of the Prince Charles Mountains–Prydz Bay region with inset showing its location in East Antarctica [XL1](modified after Fitzsimons (2003), Mikhalsky et al. (2001a)). **b**, Geological map of the Grove Mountains showed on a remote sensing image (modified after Liu et al. (2009a)).

2 Geological background

The Grove Mountains are made up of 64 nunataks of different sizes, which are spread over an area of approximately 3200 km^2. The bedrock in this area consists mainly of high-grade metamorphic rocks and abundant intrusive charnockites and granites (Figure 1b). The metamorphic rocks are dominated by felsic orthogneisses and mafic granulites, with minor quartzofeldspathic and pelitic paragneisses and calc-silicate rocks (Liu et al., 2003b, 2002). Peak *P-T* conditions of high-grade rocks are estimated at 6.1–6.7 kbar and 850ºC (Liu et al., 2003b), which are very similar to those obtained for rocks from Prydz Bay. The protoliths of felsic orthogneisses and mafic granulites were emplaced at ~920–910 Ma, and then experienced metamorphism at ~550–535 Ma (Liu et al., 2007a; Zhao et al., 2003). In addition, detrital zircons from a paragneiss record a magmatic age of ~2080 Ma and a metamorphic age of ~2050 Ma (Liu et al., 2007a). Charnockites and granites were emplaced at 547–501 Ma (Liu et al., 2006; Zhao et al., 2000).

Lateral moraines occur widely on glaciers in the Grove Mountains and are particularly concentrated in the area near the Mason Peaks, Wilson Ridge, Mount Harding and Gale Escarpment. A number of medium-pressure paragneisses and high-pressure pelitic and mafic granulites, which are distinct from the bedrock, were identified from the glacial

moraines and were inferred to have originated from the Grove Subglacial Highlands with an area of about 200 × 300 km^2 (Chen et al., 2018; Wang et al., 2016a, 2016b; Liu et al., 2009a). The deposition ages of paragneiss precursors were inferred to be younger than ~1090–940 Ma (Wang et al., 2016a), and high-pressure metamorphism was dated at ~560–540 Ma (Chen et al., 2018; Wang et al., 2016b; Liu et al., 2009a). The *P-T* path calculated for high-pressure granulites involved peak metamorphic conditions of 11.6–14.0 kbar and 770–840°C, and a subsequent near-isothermal decompression of 6 kbar (Chen et al., 2018; Liu et al., 2009a). These data provide evidence for a collisional tectonic setting for the Pan-African-aged event in the Grove Subglacial Highlands.

3 Samples and analytical techniques

3.1 Sample descriptions

Three garnet-bearing gneisses from the northern Grove Mountains were selected for a geochronological study. Sample BP2-3 is a typical pelitic paragneiss collected from Bryse Peaks. The paragneiss, together with quartzofeldspathic paragneiss and banded mafic granulite, constitutes a strongly foliated layer of 50 m thick sandwiched between layers of felsic orthogneiss (Figure 2a). It has mineral

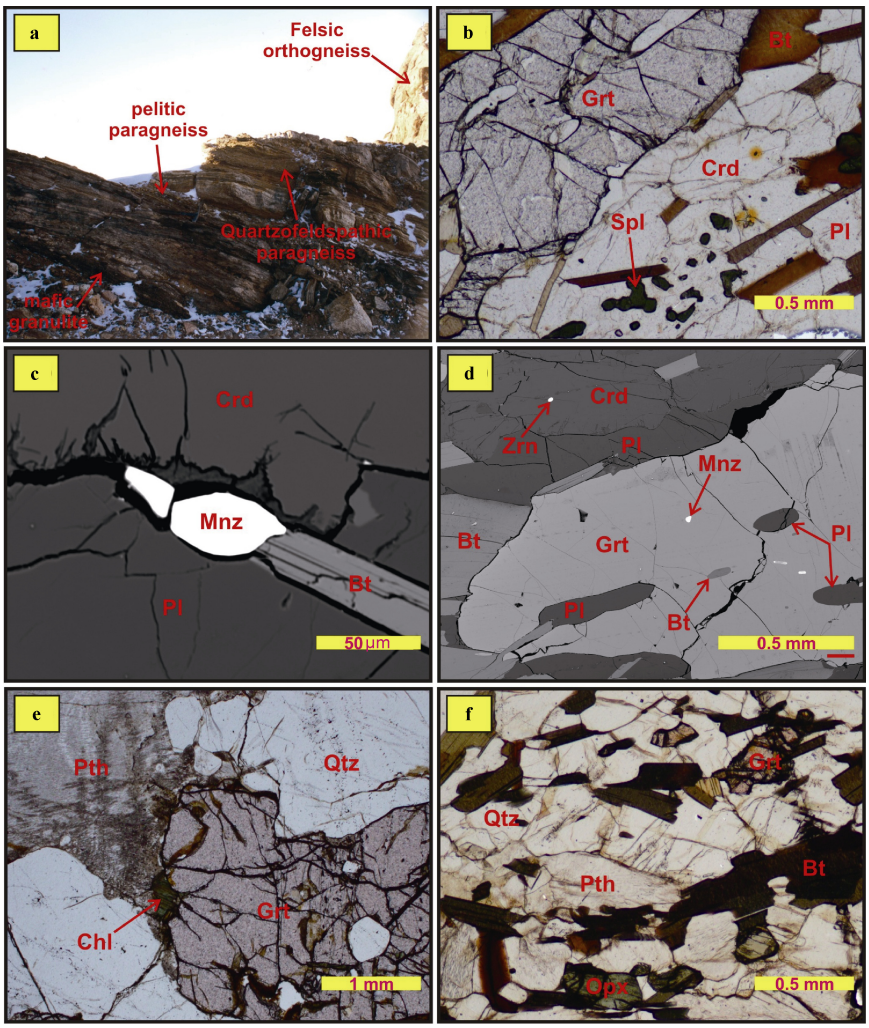

Figure 2 Photograph, photomicrographs and BSE images showing the field relationships and mineral assemblages of para- and orthogneisses from the Grove Mountains. **a**, Field relationships of felsic orthogneiss, mafic granulite and pelitic and quartzofeldspathic paragneiss from Bryse Peaks. **b**, Photomicrograph (plane-polarized light) of the mineral assemblage of inequigranular garnet + biotite + cordierite + plagioclase + spinel in pelitic paragneiss sample BP2-3 from Bryse Peaks. **c**, BSE image of monazite occurring as an intergranular phase among biotite, cordierite and plagioclase in sample BP2-3. **d**, BSE image of monazite occurring as an inclusion in garnet in sample BP2-3. **e**, Photomicrograph (plane-polarized light) of the mineral assemblage of coarse-grained garnet + perthite + quartz with a small chlorite flake in felsic orthogneiss sample WR1-2 from Wilson Ridge. **f**, Photomicrograph (plane-polarized light) of the mineral assemblage of fine-grained garnet + orthopyroxene + biotite + perthite + quartz in quartzofeldspathic paragneiss sample WR1-4 from the Wilson Ridge. Mineral abbreviations: Bt–biotite, Chl–chlorite, Crd–cordierite, Grt–garnet, Mnz–monazite, Opx–orthopyroxene, Pl–plagioclase, Pth–perthite, Qtz–quartz, Spl–spinel, Zrn–zircon.

assemblage of garnet (7%) + biotite (30%) + cordierite (20%) + plagioclase (40%) + spinel (3%) (Figure 2b), with minor ilmenite, zircon and monazite. An Al_2SiO_5 phase (sillimanite?) was identified as tiny inclusion in cordierite using backscattered electron (BSE) imaging. The grain size of garnet porphyroblasts ranges from 1 to 3 mm, but other minerals are mostly <1 mm. Monazite commonly occurs as an intergranular phase (Figure 2c), or as inclusions in garnet (Figure 2d), biotite, cordierite and plagioclase. It appears in textural equilibrium with major minerals in the rock.

Sample WR1-2 was taken from a garnet-rich domain of the felsic orthogneisses from Wilson Ridge. The rock is relatively coarse-grained and consists of garnet (8%), biotite (2%), plagioclase (10%), perthite (45%) and quartz (35%) (Figure 2e). Garnet is subhedral or anhedral, with grain sizes of 2–5 mm. It commonly contains inclusions of quartz. The felsic orthogneiss generally experienced low-grade alteration. Biotite was partially or entirely replaced by chlorite. Randomly oriented muscovite has grown in small amount along the margins of some perthite and plagioclase grains.

Sample WR1-4 is a fine-grained quartzofeldspathic paragneiss collected also from Wilson Ridge. This paragneiss occurs as layers of 5–200 cm wide in felsic orthogneiss, and was commonly intruded by thin pegmatite veins, which are parallel to the regional gneissosity of the paragneiss. The rock shows near-equigranular textures, composed of garnet (1%), orthopyroxene (8%), biotite (25%), plagioclase (5%), perthite (45%), quartz (15%) and ilmenite (1%) (Figure 2f). Garnet is anhedral, with grain sizes ranging from 0.2 to 1 mm. Orthopyroxene is subhedral and, in some cases, is concentrated in some domains.

3.2 Analytical techniques

U-Th-Pb monazite analyses were conducted using a Cameca IMS–1280 large-radius SIMS at the Institute of Geology and Geophysics, Chinese Academy of Sciences, Beijing. Prior to analysis, monazite was extracted using conventional techniques, including crushing, sieving, heavy liquid separation and handpicking. The resulting monazite grains were then mounted in epoxy discs along with a standard monazite RW-1 (Ling et al., 2016) and polished to expose the grain centers. Internal structures of monazite were revealed by BSE imaging. For the SIMS analyses, the instrument descriptions and analytical procedures are the same as those described by Li et al. (2013). The primary O^{2-} ion beam spot is about 20 μm in size. Positive secondary ions were extracted with a 10 kV potential. In the secondary ion beam optics, a 60 eV energy window was used, together with a mass resolution of ~5400 (at 10% peak height) to separate Pb^+ peaks from isobaric interferences. A single electron multiplier was used in ion-counting mode to measure secondary ion beam intensities by peak jumping mode. Each measurement consists of 7 cycles. Pb/U ratio, U and Th concentrations were calibrated against monazite RW-1 [Pb/U age=904.15 ± 0.26 Ma, Th=11.8 ± 0.5% (1σ), Th/U=42.5 ± 1.5 (1σ)]. A long-term uncertainty of 1.5% (1 RSD) for $^{206}Pb/^{238}U$ measurements of the standard monazite was propagated to the unknowns (Li et al., 2010). Common Pb was corrected using the ^{207}Pb-based method (Li et al., 2013; Williams, 1998), with the terrestrial lead isotope composition at corresponding ages (Stacey and Kramers, 1975). Ages were calculated with the ISOPLOT software (Ludwig, 2001).

Trace element analyses of monazite were carried out using laser ablation inductively coupled plasma mass spectrometry (LA–ICP–MS) at the Wuhan Sample Solution Analytical Technology Co., Ltd., Wuhan, China. Detailed operating conditions for the laser ablation system and the ICP–MS instrument and data reduction are the same as described by Zong et al. (2017). Laser sampling was performed using a GeolasPro laser ablation system that consists of a COMPexPro 102 ArF excimer laser (wavelength of 193 nm and maximum energy of 200 mJ) and a MicroLas optical system. An Agilent 7700e ICP–MS instrument was used to acquire ion-signal intensities. Helium was applied as a carrier gas. Argon was used as the make-up gas and mixed with the carrier gas via a T-connector before entering the ICP. A "wire" signal smoothing device is included in this laser ablation system (Hu et al., 2015). The spot size and frequency of the laser were set to 24 μm and 5 Hz, respectively. Trace element compositions of monazite were calibrated against various reference materials (BHVO-2G, BCR-2G and BIR-1G) without using an internal standard (Liu et al., 2008). Each analysis incorporated a background acquisition of approximately 20–30 s followed by 50 s of data acquisition from the sample. An Excel-based software ICPMSDataCal was used to perform off-line selection and integration of background and analyzed signals, time-drift correction and quantitative calibration for trace element analyses (Liu et al., 2008).

Sm-Nd mineral-whole-rock isotopic analyses were performed using a 7-collector Finnigan MAT–262 mass spectrometer at the Université de Rennes 1, France. The analytical procedures are similar to those reported by Jahn et al. (1996). Sm-Nd isochron ages were calculated using the program ISOPLOT 2.06 of Ludwig (1999). Input errors (2σ) used in age calculations are $^{147}Sm/^{144}Nd$=0.2% and $^{143}Nd/^{144}Nd$=0.005%. The quoted errors in isochron ages represent two standard deviations (2σ). Sm-Nd model ages (T_{DM}) were calculated in two ways. The one-stage depleted mantle model age (T_{DM}^1) is calculated assuming a linear isotopic evolution of the depleted mantle reservoir from $\varepsilon_{Nd}(T)$=0 at 4.56 Ga to +10 at the present. The two-stage model age (T_{DM}^2) is obtained assuming that the protolith of the granitic magmas has a Sm/Nd ratio of the average continental crust (Keto and Jacobsen, 1987). Nd isotopic normalization parameters ($^{147}Sm/^{144}Nd$=0.2137, $^{143}Nd/^{144}Nd$=0.51315) used for the calculation of model ages are the same as Liu et al. (2006).

4 Results

4.1 U-Th-Pb monazite dating

Monazites from pelitic paragneiss sample BP2-3 are ovoid or irregular in shape, with grain sizes ranging from 30 to 200 μm. Most monazite grains show a relatively dark core and a bright rim in BSE images (Figure 3), but some small ones are homogeneous. Eighteen SIMS spot analyses were performed on 12 monazite cores and 6 rims (Table 1). Th and U concentrations are quite variable and indistinguishable between cores and rims, with Th=2.6%–16.1%, U=0.42%–1.80%, and Th/U ratios=2.8–28.4. However, the cores yield relatively old $^{206}Pb/^{238}U$ ages ranging from 539.3 ± 8.2 to 509.5 ± 7.5 Ma, whereas the rims produce younger ages from 518.1 ± 7.6 to 498.6 ± 7.3 Ma. All these data points give a weighted mean $^{206}Pb/^{238}U$ age of 518 ± 5 Ma (MSWD=1.7) (Figure 4), which is in good agreement with the weighted mean $^{208}Pb/^{232}Th$ age of 518 ± 3 Ma (MSWD=1.3; excluding spot 14 with an older age of 551.7 ± 5.9 Ma). If calculated separately, 12 core and 6 rim analyses yield weighted mean $^{206}Pb/^{238}U$ ages of 523 ± 4 Ma (MSWD=0.92) and 508 ± 6 Ma (MSWD=0.85), respectively.

Eighteen LA–ICP–MS trace element analyses were also undertaken on all dated monazite domains (Table 2). As is the case with Th and U concentrations, trace element concentrations show wide variation that appears unrelated to the zoning visible in the BSE images. Dark cores show Y abundances of 0.73%–3.74% and total rare earth element (REE) contents of 49.95%–58.35%. The chondrite-normalized REE patterns are enriched in light REE (La_N/Yb_N=54–801) and have variable negative Eu anomalies (Eu/Eu*=0.03–0.32) (Figure 5). By contrast, bright rims have Y abundances of 0.85%–3.69% and total REE contents of 51.30%–55.31%. They also display highly fractionated REE patterns (La_N/Yb_N=55–715) and markedly negative Eu anomalies (Eu/Eu*=0.03–0.08).

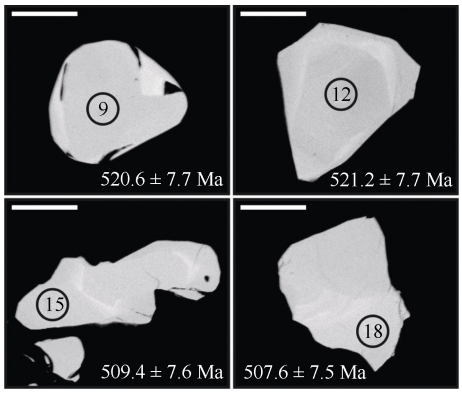

Figure 3 Representative BSE images of monazites from pelitic paragneiss sample BP2-3. All monazites showing a relatively dark core and a bright rim. Circles with numbers are SIMS analytical spots with their identification numbers. Ages are given with errors of 1σ. Scale bars are 50 μm.

Table 1 SIMS U-Pb analyses of monazites from sample BP2-3

Spot	U/(ppm)	Th/(ppm)	Th/U	Isotopic ratios						Ages/Ma			
				$^{208}Pb/^{232}Th$	±σ/(%)	$^{238}U/^{206}Pb$	±σ/(%)	$^{207}Pb/^{206}Pb$	±σ/(%)	$^{208}Pb/^{232}Th$	±σ	$^{206}Pb/^{238}U$	±σ
Dark core													
1	0.52	3.0	5.8	0.02592	1.31	11.823	1.52	0.05896	0.55	517.3	6.7	522.6	7.8
2	0.77	8.0	10.3	0.02578	1.14	11.927	1.54	0.05858	0.46	514.5	5.8	518.5	7.8
3	0.53	11.1	21.1	0.02618	1.08	11.832	1.50	0.05957	0.60	522.4	5.6	521.9	7.7
4	0.42	8.7	20.6	0.02665	1.12	11.438	1.56	0.05966	0.60	531.7	5.9	539.3	8.2
5	0.43	6.1	14.1	0.02643	1.23	11.638	1.58	0.05846	0.61	527.3	6.4	531.1	8.2
6	0.67	8.2	12.3	0.02597	1.10	11.877	1.50	0.05820	0.50	518.1	5.6	520.8	7.7
7	0.71	3.1	4.3	0.02593	1.12	11.721	1.51	0.05824	0.51	517.4	5.7	527.6	7.8
8	0.48	13.7	28.4	0.02594	1.09	11.991	1.50	0.05910	0.69	517.6	5.6	515.4	7.6
9	0.63	11.3	17.9	0.02596	1.03	11.875	1.51	0.05869	0.65	518.1	5.3	520.6	7.7
10	0.42	10.0	24.0	0.02546	1.11	12.136	1.50	0.05888	0.62	508.1	5.6	509.5	7.5
11	0.53	2.6	4.9	0.02598	1.04	11.757	1.51	0.05908	0.53	518.5	5.3	525.5	7.7
12	0.70	5.0	7.2	0.02593	1.08	11.863	1.50	0.05862	0.58	517.4	5.5	521.2	7.7
Bright rim													
13	0.84	16.1	19.2	0.02614	1.09	12.306	1.51	0.05824	0.52	521.5	5.6	503.0	7.4
14	0.74	9.6	13.0	0.02767	1.08	11.946	1.51	0.05793	0.61	551.7	5.9	518.1	7.6
15	0.51	10.4	20.3	0.02581	1.06	12.149	1.51	0.05827	1.22	515.2	5.4	509.4	7.6
16	1.80	5.0	2.8	0.02575	1.07	12.069	1.50	0.05814	0.37	513.8	5.4	512.8	7.5
17	0.50	9.2	18.6	0.02654	1.05	12.421	1.50	0.05808	0.64	529.5	5.5	498.6	7.3
18	0.63	12.2	19.2	0.02541	1.07	12.184	1.52	0.05882	0.80	507.1	5.3	507.6	7.5

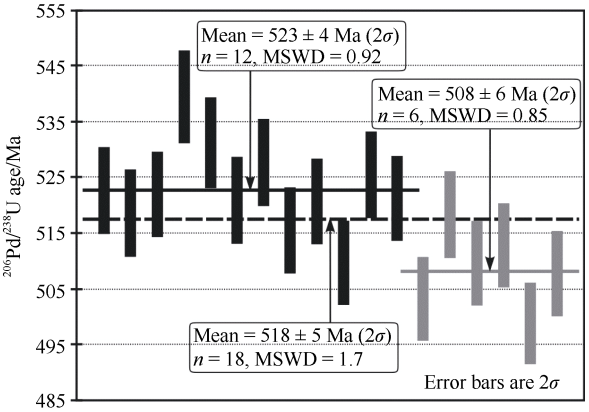

Figure 4 Distribution plots of $^{206}Pb/^{238}U$ ages of monazites from pelitic paragneiss sample BP2-3.

4.2 Sm-Nd mineral-whole-rock dating

Coarse-grained garnet, plagioclase and perthite from felsic orthogneiss sample WR1-2 and fine-grained garnet, orthopyroxene, biotite, plagioclase and perthite from quartzofeldspathic paragneiss sample WR1-4 were separated for Sm-Nd isotopic analyses together with whole-rock powder (Table 3). The obtained mineral-whole-rock isochron ages are 536 ± 3 Ma (MSWD=0.67) for sample WR1-2 (Figure 6), and 507 ± 30 Ma (MSWD=4.6) for sample WR1-4 (Figure 7). The initial $^{143}Nd/^{144}Nd$ ratios (I_{Nd}) are 0.511450 ± 0.000015 and 0.51130 ± 0.00005, respectively. In addition, the whole-rock analyses yield an initial ε_{Nd} value [ε_{Nd} (T)] of –9.9 and a two-stage Nd model age (T_{DM}^2) of 2.11 Ga for sample WR1-2, and ε_{Nd} (T) of –13.3 and T_{DM}^2 of 2.38 Ga for sample WR1-4.

Table 2 Trace element analyses (in ppm) of monazites from sample BP2-3

Spot	Y	La	Ce	Pr	Nd	Sm	Eu	Gd	Tb	Dy	Ho	Er	Tm	Yb	Lu	REE	La_N/Yb_N	Eu/Eu*
Dark core																		
1	23534	136909	258375	27893	109637	18459	1059	12986	1596	7357	951	1892	195	786	63.3	578157	125	0.20
2	37363	116057	229758	25559	104071	18814	258	15103	1916	9796	1418	3326	366	1555	135	528133	54	0.05
3	8507	125150	234074	27549	101963	17809	298	11770	1037	3429	353	581	48.6	181	15.4	524257	495	0.06
4	20494	119467	219950	23542	92970	16577	1592	13004	1649	7405	894	1624	151	590	44.5	499461	145	0.32
5	25331	127808	243589	26721	105074	18924	1192	14352	1750	8041	1020	2053	206	825	67.5	551624	111	0.21
6	24377	123908	231248	25337	103996	18983	566	14881	1716	7525	993	1990	196	818	71.9	532230	109	0.10
7	29397	133515	253312	27428	108100	19120	1020	14257	1830	9052	1168	2410	249	1035	80.7	572576	93	0.18
8	11931	112212	224138	25094	104230	18508	236	12278	1182	4299	498	912	83.9	326	28.0	504025	247	0.04
9	7303	121124	234086	26402	109630	19336	203	12662	1083	3341	314	450	32.7	109	8.11	528782	801	0.04
10	11607	111793	230632	26675	111988	20746	182	14000	1323	4664	489	779	55.8	179	12.8	523519	447	0.03
11	26233	135209	261569	28237	111420	18980	1028	13105	1649	7755	1039	2195	238	1019	84.0	583528	95	0.19
12	27904	132540	251065	27119	110141	18944	381	14433	1748	7995	1113	2389	250	1055	95.0	569267	90	0.07
Bright rim																		
13	31911	126043	239627	26608	108269	19651	440	15884	1929	9019	1235	2475	232	886	70.6	552367	102	0.07
14	36874	115560	225579	25205	102625	18702	433	15021	1954	9894	1419	3270	358	1497	128	521645	55	0.08
15	26453	111598	220061	24908	104287	19846	242	16627	2070	9658	1147	1921	146	466	33.4	513011	172	0.04
16	29890	104601	231013	27695	116089	28589	226	25269	3043	12633	1304	2039	139	398	26.4	553064	188	0.03
17	14706	113228	235225	27327	113358	21375	194	15748	1631	6147	663	1038	74.7	236	16.8	536260	344	0.03
18	8531	109968	228766	26893	115419	21453	157	13800	1196	3805	370	533	36.1	110	7.22	522514	715	0.03

5 Discussion and conclusions

5.1 Interpretation of U-Th-Pb monazite and Sm-Nd mineral-whole-rock ages

Since the Pb closure temperature of monazite could exceed 900ºC (Cherniak et al., 2004), this accessory mineral was frequently used to date medium- to high-grade metamorphism. Unfortunately, because the internal zoning, as shown in BSE images, of monazites from sample BP2-3 does not match the variation of trace elements (particularly Y contents), the growth relationship between monazite and garnet was not established in this study. The U-Pb age of 523 ± 4 Ma obtained for monazite cores is roughly in accord with the ages (~535–525 Ma) of regional medium-pressure granulite-facies metamorphism in the eastern Amery Ice Shelf–Prydz Bay region (Liu et al., 2009b, 2007b; Kelsey et al., 2007; Ziemann et al., 2005; Fitzsimons et al., 1997; Zhang et al., 1996) and retrograde metamorphic age (~530 Ma) of high-pressure mafic granulites from the Grove Mountains (Liu et al., 2009a). Coupled with the coexistence of monazite and cordierite in

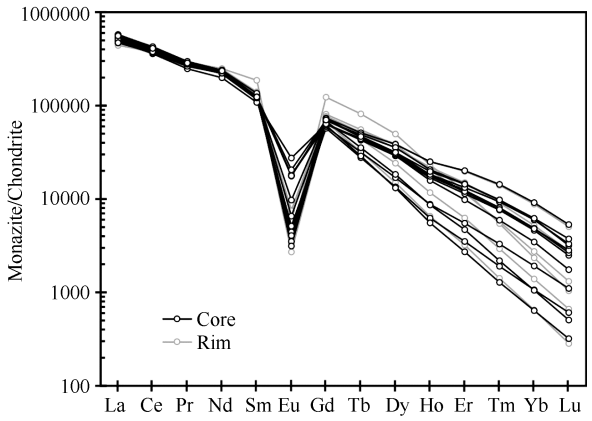

Figure 5 Chondrite-normalized REE patterns of monazites from pelitic paragneiss sample BP2-3. Chondrite-normalization values are from Sun and McDonough (1989).

the sample, this age is taken to represent the approximate time of medium- to low-pressure granulite-facies metamorphism in the Grove Mountains. Based on geochemical data of zircon and associated minerals in high-grade rocks from the Rauer Group, the zircon rim age of ~510 Ma was interpreted as the time of post-peak fluid infiltration (Harley and Kelly, 2007). The age of 508 ± 6 Ma obtained for monazite rims could also be attributed to post-peak infiltration, since hydrothermal alteration under greenschist-facies conditions has been recognized in sample WR1-2 and some other rocks from the Grove Mountains (Liu et al., 2009a).

The Nd closure temperature of garnet is generally inferred to be ~700–750ºC (Ganguly et al., 1998), although there is a difference between fast and slowly cooled terranes. Therefore, garnet-based Sm-Nd isochron age commonly reflect the time of cooling of garnet through its closure

Table 3 Sm-Nd isotopic compositions of samples WR1-2 and WR1-4

Whole-rock and mineral	Sm /(ppm)	Nd /(ppm)	$^{147}Sm/^{144}Nd$	$^{143}Nd/^{144}Nd$	$\pm 2\sigma m$	Isochron age/Ma	Initial ratio (metamorphic)	$\varepsilon_{Nd}(T)$	T_{DM}^{1} /Ga	T_{DM}^{2} /Ga
Sample WR1-2 (felsic orthogneiss)										
Whole-rock	0.548	3.140	0.1054	0.511821	4	536±3	0.511450±15	−9.9	1.87	2.11
Garnet	7.429	2.341	1.9214	0.518202	3					
Plagioclase	1.308	8.642	0.0915	0.511763	4					
Perthite	0.213	1.946	0.0662	0.511695	4					
Sample WR1-4 (quartzofeldspathic paragneiss)										
Whole-rock	5.241	29.36	0.1079	0.511656	4					
Garnet	8.144	9.211	0.5346	0.513067	4					
Orthopyroxene	1.130	2.919	0.2340	0.512113	4	507±30	0.51130±5	−13.3	2.14	2.38
Biotite	1.358	7.434	0.1104	0.511630	3					
Plagioclase	2.909	19.13	0.0919	0.511623	3					
Perthite	2.692	15.35	0.1060	0.511652	6					

temperature. The age of 536 ± 3 Ma obtained for coarse-grained sample WR1-2 is similar to the Sm-Nd garnet–whole-rock ages of 538–522 Ma obtained for high-pressure mafic granulites from the Grove Mountains (Liu et al., 2009a). Considering the relatively weak effect of Nd diffusion for large garnet grains, we infer this age quite close to the age of regional metamorphism in the Grove Mountains. In contrast, the age of 507 ± 30 Ma obtained for fine-grained sample WR1-4 is obviously young and has a large uncertainty, indicating a strong Nd diffusion of garnet. Therefore, this age is interpreted as the cooling age of the rock. In fact, this age is also comparable to the monazite rim age mentioned above, and U-Pb ages (~510 Ma) of rutile and titanite and $^{40}Ar/^{39}Ar$ ages (~510–490 Ma) of hornblende and biotite from rocks in the Grove Mountains (Mikhalsky et al., 2001b; Hu et al., unpublished data). Similar Sm-Nd ages (~515–490 Ma) were widely reported in the eastern Amery Ice Shelf–Prydz Bay region (Liu et al., 2007b; Hensen and Zhou, 1995).

5.2 Implications for a Pan-African-aged mono-metamorphic terrane in the Prydz Belt

The Prydz Belt has long been thought to be a typical polymetamorphic belt that underwent both Grenville-aged and Pan-African-aged high-grade metamorphism (Dirks and Wilson, 1995). The earliest geochronological evidence for the Grenville-aged metamorphism in the Prydz Belt comes from garnet-bearing mafic granulites from the Søstrene Island. Hensen and Zhou (1995) obtained five Sm-Nd garnet–whole-rock isochron ages for these rocks, and the oldest one of 988 ± 12 Ma was interpreted as the age of the

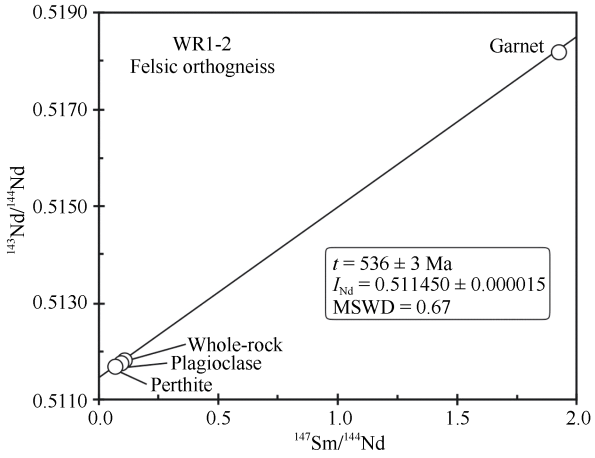

Figure 6 Sm-Nd mineral-whole-rock isochron diagram for felsic orthogneiss sample WR1-2.

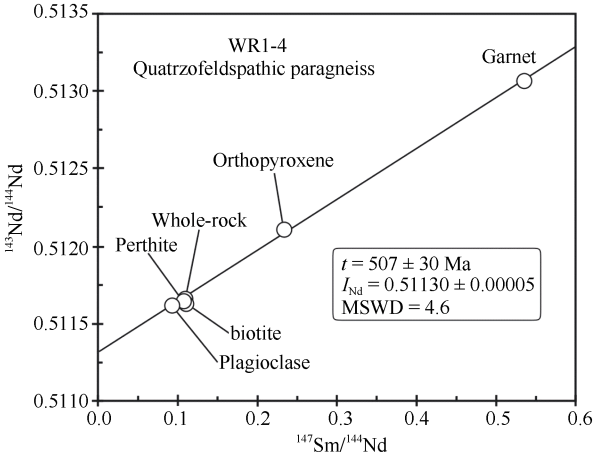

Figure 7 Sm-Nd mineral-whole-rock isochron diagram for quartzofeldspathic paragneiss sample WR1-4.

metamorphic event. Subsequently, U-Pb or (U + Th)-Pb monazite ages of ~1030–820 Ma were reported from some metapelites from the Rauer Group and Bolingen Islands (Kelsey et al., 2007; Kinny 1998). Moreover, further detailed SHRIMP U-Pb zircon dating for felsic orthogneisses and mafic granulites from the eastern Amery Ice Shelf–Prydz Bay region demonstrated a widespread existence of this event in the basement of the Prydz Belt (Liu et al., 2014, 2009b, 2007b; Grew et al., 2012; Wang et al., 2008; Carson et al., 2007).

As mentioned previously, the Grove Mountains are an inland continuation of the Prydz Belt. However, the Grenville-aged metamorphic event was not identified from both bedrock and glacial moraines using U-Pb zircon geochronology (Chen et al., 2018; Hu et al., 2016; Wang et al., 2016a, 2016b; Liu et al., 2009a, 2007a). The present U-Th-Pb monazite and Sm-Nd mineral-whole-rock dating for para- and orthogneisses from bedrock have also not manifested the existence of this earlier event. More importantly, the Pan-African-aged metamorphic zircon rims grew directly on magmatic zircon cores of ~920–910 Ma in felsic orthogneisses and mafic granulites, and the Paleoproterozoic detrital zircons from pelitic paragneiss sample BP2-3 uniquely record an imprecise U-Pb lower intercept age of ~500 Ma (Liu et al., 2007a). All these data taken together suggest that the Grove Mountains, while a part of the Prydz Belt, were affected by a single Pan-African-aged metamorphic event. Taking into account the absence of the Grenville-aged metamorphic event in the Archean Rauer Group (Hokada et al., 2016; Kelsey et al., 2007, 2003), it can be concluded that some terranes in the Prydz Belt were not involved in the Grenville-aged orogeny.

A Pan-African-aged monometamorphic terrane in the Grove Mountains provides much better constraints on the nature of the Prydz Belt. The available petrological and geochronological data obtained for bedrock and glacial moraines from the Grove Mountains indicate a Pan-African -aged tectonometamorphic evolution as follows. (1) The crustal rocks were buried to depths of ~40–50 km and underwent high-pressure granulite-facies metamorphism accompanied by charnockitic intrusion at ~560–540 Ma. (2) The high-pressure rocks were exhumed to mid-upper crustal levels and suffered regional medium- to low-pressure granulite-facies metamorphism with concomitant charnockitic and granitic intrusion at ~530 Ma. (3) Crustal extension and greenschist-facies metamorphic overprinting, in association with the widespread emplacement of granites and granitic dykes, took place at ~510–490 Ma. This may reflect a complete orogenic process from continental collision to extensional collapse.

Acknowledgments We would like to thank Liu Xiaohan, Li Jinyan and Huo Dongmin for assistance during field work. The field work was carried out during the 15th Chinese National Antarctic Research Expedition during 1998–1999. We gratefully acknowledge logistic support from the Chinese Arctic and Antarctic Administration and financial support from the National Natural Science Foundation of China (Grant no. 41530209) and the Central Public-Interest Scientific Institution Basal Research Fund (Grant no. JYYWF201819). Critical reviews by E. S. Grew and E. V. Mikhalsky substantially improved the manuscript.

References

Boger S D. 2011. Antarctica—before and after Gondwana. Gondwana Res, 19: 335-371.

Carson C J, Grew E S, Boger S D, et al. 2007. Age of boron- and phosphorus-rich paragneisses and associated orthogneisses, Larsemann Hills: new constraints from SHRIMP U-Pb zircon geochronology//Cooper A K, Raymond C R. A keystone in a changing world–Online Proceedings of the 10th ISAES. USGS Open File Report 2007-1047, Extended Abstract 003, 4.

Carson C J, Fanning C M, Wilson C J L. 1996. Timing of the Progress Granite, Larsemann Hills: evidence for Early Palaeozoic orogenesis within the East Antarctica Shield and implications for Gondwana

assembly. Aust J Earth Sci, 43: 539-553.

Chen L Y, Wang W, Liu X C, et al. Metamorphism and zircon U-Pb dating of high-pressure pelitic granulites from glacial moraines in the Grove Mountains, East Antarctica. Adv Polar Sci, 2018, 29(2): 118-134, doi:10.13679/j.advps.2018.2.00118.

Cherniak, D J, Watson E B, Grove M, et al. 2004. Pb diffusion in monazite: a combined RBS/SIMS study. Geochim Cosmochim Acta, 68: 829-840.

Dirks P H G M, Wilson C J L. 1995. Crustal evolution of the East Antarctic mobile belt in Prydz Bay: continental collision at 500 Ma? Precambr Res, 75: 189-207.

Fitzsimons I C W. 2003. Proterozoic basement provinces of southern and southwestern Australia, and their correlation with Antarctica//Yoshida M, Windley B, Dasgupta S. Proterozoic East Gondwana: Supercontinent assembly and breakup. Geol Soc London Spec Publ, 206: 93-130.

Fitzsimons I C W. 2000. A review of tectonic events in the East Antarctic Shield and their implications for Gondwana and earlier supercontinents. J Afr Earth Sci, 31: 3-23.

Fitzsimons I C W, Kinny P D, Harley S L. 1997. Two stages of zircon and monazite growth in anatectic leucogneiss: SHRIMP constraints on the duration and intensity of Pan-African metamorphism in Prydz Bay, East Antarctica. Terra Nova, 9: 47-51.

Ganguly J, Tirone M, Hervig R L. 1998. Diffusion kinetics of samarium and neodymium in garnet, and a method for determining cooling rates of rocks. Science, 281: 805-807.

Grew E S, Carson C J, Christy A G, et al. 2012. New constraints from U-Pb, Lu-Hf and Sm-Nd isotopic data on the timing of sedimentation and felsic magmatism in the Larsemann Hills, Prydz Bay, East Antarctica. Precambr Res, 206-207: 87-108.

Harley S L. 2003. Archaean-Cambrian crustal development of East Antarctica: metamorphic characteristics and tectonic implications// Yoshida M, Windley B, Dasgupta S. Proterozoic East Gondwana: Supercontinent assembly and breakup. Geol Soc London Spec Publ, 206: 203-230.

Harley S L, Kelly N M. 2007. The impact of zircon–garnet REE distribution data on the interpretation of zircon U-Pb ages in complex high-grade terrains: an example from the Rauer Islands, East Antarctica. Chem Geol, 241: 62-87.

Hensen B J, Zhou B. 1995. A Pan-African granulite facies metamorphic episode in Prydz Bay, Antarctica: evidence from Sm-Nd garnet dating. Aust J Earth Sci, 42: 249-258.

Hokada T, Harley S L, Dunkley D J, et al. 2016. Peak and post-peak development of UHT metamorphism at Mather Peninsula, Rauer Island: zircon and monazite U-Th-Pb and REE chemistry constraints. J Mineral Petrol Sci, 111: 89-103.

Hu J M, Ren M H, Zhao Y, et al. 2016. Source region analyses of the morainal detritus from the Grove Mountains: evidence from the subglacial geology of the Ediacaran-Cambrian Prydz Belt of East Antarctica. Gondwana Res, 35: 164-179.

Hu Z C, Zhang W, Liu Y S, et al. 2015. “Wave” signal smoothing and mercury removing device for laser ablation quadrupole and multiple collector ICP-MS analysis: application to lead isotope analysis. Anal Chem, 87: 1152-1157.

Jahn B-M, Cornichet J, Cong B L, et al. 1996. Ultrahigh ε_{Nd} eclogites from an UHP metamorphic terrane of China. Chem Geol, 127: 61-79.

Kelsey D E, Hand M, Clark C, et al. 2007. On the application of *in situ* monazite chemical geochronology to constraining *P-T-t* histories in high-temperature (>850°C) polymetamorphic granulites from Prydz Bay, East Antarctica. J Geol Soc London, 164: 667-683.

Kelsey D E, Powell R, Wilson C J L, et al. 2003. (Th + U)-Pb monazite ages from Al-Mg-rich metapelites, Rauer Group, East Antarctica. Contrib Mineral Petrol, 146: 326-340.

Keto L S, Jacobsen S B. 1987. Nd and Sr isotopic variations of Early Paleozoic oceans. Earth Planet Sci Lett, 84: 27-41.

Kinny P D. 1998. Monazite U-Pb ages from east Antarctic granulites: comparisons with zircon U-Pb and garnet Sm-Nd ages. Geological Society of Australia, Abstracts, 49: 250.

Li Q L, Li X H, Lan Z W, et al. 2013. Monazite and xenotime U-Th-Pb geochronology by ion microprobe: dating highly fractionated granites at Xihuashan tungsten mine, SE China. Contrib Mineral Petrol, 166: 65-80.

Li Q L, Li X H, Liu Y, et al. 2010. Precise U-Pb and Pb-Pb dating of Phanerozoic baddeleyite by SIMS with oxygen flooding technique. J Anal At Spectrom, 25: 1107-1113.

Ling X X, Huyskens M H, Li Q L, et al. 2016. Monazite RW-1: a homogenous natural reference material for SIMS U-Pb and Th-Pb isotopic analysis. Miner Petrol, 111: 163-172, doi:10.1007/s00710-016-0478-7.

Liu X C, Jahn B-M, Zhao Y, et al. 2014. Geochemistry and geochronology of Mesoproterozoic basement rocks from the eastern Amery Ice Shelf and southwestern Prydz Bay, East Antarctica: implications for a long-lived magmatic accretion in a continental arc. Am J Sci, 314: 508-547.

Liu X C, Zhao Y, Hu J M, et al. 2013. The Grove Mountains: a typical Pan-African metamorphic terrane in the Prydz Belt, East Antarctica. Chin J Polar Res, 25: 7–24 (in Chinese with English abstract).

Liu X C, Hu J M, Zhao Y, et al. 2009a. Late Neoproterozoic/Cambrian high-pressure mafic granulites from the Grove Mountains, East Antarctica: *P-T-t* path, collisional orogeny and implications for assembly of East Gondwana. Precambr Res, 174: 181-199.

Liu X C, Zhao Y, Song B, et al. 2009b. SHRIMP U-Pb zircon geochronology of high-grade rocks and charnockites from the eastern Amery Ice Shelf and southwestern Prydz Bay, East Antarctica: constraints on Late Mesoproterozoic to Cambrian tectonothermal events related to supercontinent assembly. Gondwana Res, 16: 342-361.

Liu X C, Jahn B-M, Zhao Y, et al. 2007a. Geochemistry and geochronology of high-grade rocks from the Grove Mountains, East Antarctica: evidence for an Early Neoproterozoic basement metamorphosed during a single Late Neoproterozoic/Cambrian tectonic cycle. Precambr Res, 158: 93-118.

Liu X C, Zhao Y, Zhao G C, et al. 2007b. Petrology and geochronology of granulites from the McKaskle Hills, eastern Amery Ice Shelf, Antarctica, and implications for the evolution of the Prydz Belt. J Petrol, 48: 1443-1470.

Liu X C, Jahn B-M, Zhao Y, et al. 2006. Late Pan-African granitoids from the Grove Mountains, East Antarctica: age, origin and tectonic implications. Precambr Res, 145: 131-154.

Liu X H, Zhao Y, Liu X C, et al. 2003a. Geology of the Grove Mountains in East Antarctica− new evidence for the final suture of Gondwana Land. Sci China (Ser D), 46: 305-319.

Liu X C, Zhao Z R, Zhao Y, et al. 2003b. Pyroxene exsolution in mafic

granulites from the Grove Mountains, East Antarctica: constraints on the Pan-African metamorphic conditions. Eur J Mineral, 15: 55-65.

Liu X C, Zhao Y, Liu X H. 2002. Geological aspects of the Grove Mountains, East Antarctica//Gamble J A, Skinner D N B, Henrys S. Antarctica at the Close of a Millennium. R Soc New Zealand Bull, 35: 161-166.

Liu Y S, Hu Z C, Gao S, et al. 2008. In situ analysis of major and trace elements of anhydrous minerals by LA–ICP–MS without applying an internal standard. Chem Geol, 257: 34-43.

Ludwig K R. 2001. Users manual for Isoplot/Ex (v. 2.49). Berkeley Geochronology Center, Special Publication, No. 1.

Ludwig K R. 1999. Isoplot/Ex (v. 2.06)—a geochronological toolkit for Microsoft Excel. Berkeley Geochronology Center, Special Publication, No. 1a.

Mikhalsky E V, Sheraton J W, Laiba A A, et al. 2001a. Geology of the Prince Charles Mountains, Antarctica. AGSO Geosci Aust Bull, 247: 1-209.

Mikhalsky E V, Sheraton J W, Beliatsky B V. 2001b. Preliminary U-Pb dating of Grove Mountains rocks: implications for the Proterozoic to Early Palaeozoic tectonic evolution of the Lambert Glacier─Prydz Bay area (East Antarctica). Terra Antarct, 8: 3-10.

Stacey J S, Kramers J D. 1975. Approximation of terrestrial lead isotope evolution by a two-stage model. Earth Planet Sc Lett, 26: 207-221.

Sun S S, McDonough W E. 1989. Chemical and isotopic systematics of oceanic basalts: implications for mantle composition and processes//Saunders A D, Norry M J. Magmatism in the Ocean Basins. Geol Soc London Spec Publ, 42: 313-345.

Wang W, Liu X C, Zhao Y, et al. 2016a. U-Pb zircon ages and Hf isotopic compositions of metasedimentary rocks from the Grove Subglacial Highlands, East Antarctica: constraints on the provenance of protoliths and timing of sedimentation and metamorphism. Precambr Res, 275: 135-150.

Wang W, Liu X C, Zhao Y, et al. 2016b. U-Pb zircon chronology of high-pressure granulites and orthogneisses from glacial moraines in the Grove Mountains, East Antarctica. Chin J Polar Res, 28: 151-160 (in Chinese with English abstract).

Wang Y B, Liu D Y, Chung S-L, et al. 2008. SHRIMP zircon age constraints from the Larsemann Hills region, Prydz Bay, for a late Mesoproterozoic to early Neoproterozoic tectono-thermal event in East Antarctica. Am J Sci, 308: 573-617.

Williams I S. 1998. U-Th-Pb geochronology by ion microprobe. Rev Econ Geol, 7: 1-35.

Yoshida M, Jacobs J, Santosh M, et al. 2003. Role of Pan-African events in the Circum-East Antarctic Orogen of East Gondwana: a critical overview//Yoshida M, Windley B, Dasgupta S. Proterozoic East Gondwana: Supercontinent assembly and breakup. Geol Soc London Spec Publ 206: 57-75.

Zhang L S, Tong L X, Liu X H, et al. 1996. Conventional U-Pb age of the high-grade metamorphic rocks in the Larsemann Hills, East Antarctica.//Pang Z, Zhang J, Sun J. Advances in Solid Earth Sciences. Beijing: Science Press, 27-35.

Zhao Y, Liu X H, Liu X C, et al. 2003. Pan-African events in Prydz Bay, East Antarctica and its inference on East Gondwana tectonics//Yoshida M, Windley B, Dasgupta S. Proterozoic East Gondwana: Supercontinent assembly and breakup. Geol Soc London Spec Publ, 206: 231-245.

Zhao Y, Liu X C, Fanning C M, et al. 2000. The Grove Mountains, a segment of a Pan-African orogenic belt in East Antarctica. Abstract Volume of the 31th IGC, Rio de Janeiro, Brazil.

Zhao Y, Liu X H, Song B, et al. 1995. Constraints on the stratigraphic age of metasedimentary rocks from the Larsemann Hills, East Antarctica: possible implications for Neoproterozoic tectonics. Precambr Res, 75: 175-188.

Zhao Y, Song B, Wang Y B, et al. 1992. Geochronology of the late granite in the Larsemann Hills, East Antarctica//Yoshida Y, Kaminuma K, Shiraishi K. Recent progress in Antarctic earth science. Terra Scientific Publishing Company, Tokyo, 155-161.

Ziemann M A, Förster H-J, Harlov D E, et al. 2005. Origin of fluorapatite-monazite assemblages in a metamorphosed, sillimanite-bearing pegmatoid, Reinbolt Hills, East Antarctica. Eur J Mineral, 17: 567-579.

Zong K Q, Klemd R, Yuan Y, et al. 2017. The assembly of Rodinia: the correlation of early Neoproterozoic (*ca*. 900 Ma) high-grade metamorphism and continental arc formation in the southern Beishan Orogen, southern Central Asian Orogenic Belt (CAOB). Precambr Res, 290: 32-48.